Effects of Site-Directed Mutagenesis of Protolytic Residues in Subunit I of *Bacillus subtilis* aa_3-600 Quinol Oxidase. Role of Lysine 304 in Proton Translocation†

Gaetano Villani,‡ Nazzareno Capitanio,‡ Antonella Bizzoca,‡ Luigi L. Palese,‡ Valeria Carlino,‡ Maria Tattoli,‡ Philippe Glaser,§ Antoine Danchin,§ and Sergio Papa*,‡

Institute of Medical Biochemistry and Chemistry, University of Bari, Bari, Italy, and Unité de Regulation de l'Expression Génétique, Institut Pasteur, Paris Cedex, France

Received April 7, 1998; Revised Manuscript Received December 14, 1998

ABSTRACT: Various protolytic residues in subunit I of aa_3-600 quinol oxidase of the aerobic Gram-positive *Bacillus subtilis* were mutagenized to nonpolar residues. Two of the mutations, Y284F and K304L, impaired the bioenergetic function of the microorganism. The Y284F mutation suppressed the electron-transfer activity of quinol oxidase and altered its interaction with CO and H_2O_2, thus showing destruction of the binuclear domain as observed for the bo_3 quinol oxidase of *Escherichia coli*. The K304L mutation did not alter significantly the redox activity of the oxidase and its interaction with CO and H_2O_2 but suppressed the proton pumping activity of the enzyme. These results show that the K304 residue, which is invariantly conserved (as K or R) in practically all the sequences of the heme−copper oxidases so far available (around 100), is essential for the proton pumping activity of the oxidase.

The enzymes of the superfamily of heme−copper oxidases (*1, 2*) catalyze the transfer of electrons from cytochrome *c* or quinol (the latter in some prokaryotic oxidases) to dioxygen and convert redox free energy in a transmembrane electrochemical proton gradient Δp (*3*−*5*). The latter derives, in the first place, directly from the membrane anisotropy of reduction of O_2 to H_2O, whereby electrons are donated by cytochrome *c* (or quinol) at the outer P side of the membrane and protons are taken up from the inner aqueous phase (*6*). Oxidation of a quinol molecule results, in the case of quinol oxidases, in the release of two scalar protons in the outer P phase. In addition, electron flow in protonmotive oxidases is associated with proton pumping from the N to the P aqueous phase (*7, 8*).

All protonmotive heme−copper oxidases have a heme−copper (Cu_B) center where the reductive chemistry of oxygen takes place. This binuclear center is associated with subunit I, the most conserved subunit in the members of the superfamily, which in eukaryotic and prokaryotic cytochrome *c* oxidases and quinol oxidases is also associated with a low potential heme (heme *a* or *b* type) (*2*). Cytochrome *c* oxidases have an additional bimetallic Cu center (Cu_A) which serves as the entry port of electrons and is associated with subunit II, the second conserved subunit in all the members of the superfamily. In heme−copper oxidases there is a conserved third subunit, whose role is still not well understood, and supernumerary subunits whose number varies from one (in prokaryotic oxidases) up to ten in mammalian oxidases (*9*).

The aa_3-600 quinol oxidase is one of the terminal oxidases of the branched respiratory chain of the aerobic Gram-positive *Bacillus subtilis* whose genome has been completely sequenced (*10*). This organism can synthesize *a*-, *b*-, *c*-, *d*-, and *o*-type cytochromes (*11*) and, depending on the growth conditions, four terminal oxidases: the caa_3-605 cytochrome *c* oxidase, the aa_3-600 and *d*-type quinol oxidases, and a *b*- or *o*-type oxidase (*12*−*15*).

The aa_3-600 quinol oxidase of *B. subtilis* is a four-subunit enzyme encoded by the *qox* operon (*16, 17*), subunits I, II, III, and IV being respectively encoded by the genes *qoxB*, *qoxA*, *qoxC*, and *qoxD*. This oxidase is constitutively expressed when *B. subtilis* 168 is grown aerobically to the exponential phase in rich media. Using the high efficiency of homologous gene recombination in the chromosome of *B. subtilis*, our group has developed a strategy for mutational analysis of the quinol oxidase. In particular, it was found that deletion of the *qoxC* gene (subunit III) causes a defective assembly of the aa_3-600 quinol oxidase in the *B. subtilis* plasma membrane (*15;* cf. ref *18*). Deletion of the *qoxD* gene resulted in the expression of a normal content of heme aa_3-600 but in depression of its activity (*15*). This observation was confirmed by Saiki et al. (*19*), who provided evidence indicating that subunit IV assists the binding of Cu_B to subunit I during biosynthesis or assembly of the oxidase complex.

We have now extended our work to site-directed mutagenesis of specific residues in subunit I of aa_3-600 quinol oxidase of *B. subtilis* with the aim to identify aminoacids possibly involved in its protonmotive activity. Site-directed mutagenesis of subunit I of the bo_3 quinol oxidase of *Escherichia coli* (*20, 21*) and of cytochrome *c* oxidase of

† This work was financially supported by Grant 97.01167.PF49 from Biotechnologies of the Italian Research Council and by a grant from the Italian Project for Bioenergetics and Membrane Transport of MURST, Italy. G.V. was supported by a 2-month EMBO short-term fellowship (ASTF 7971) during his stay at the Pasteur Institute.

* To whom correspondence should be addressed at the University of Bari, Piazza G. Cesare, Policlinico, 70124 BARI Italy. Phone: +39-80-5478428. Fax: +39-80-5478429. E-mail: papabchm@cimedoc.uniba.it.

‡ University of Bari.

§ Institut Pasteur.

10.1021/bi980774g CCC: $18.00
Published on Web 02/05/1999

Rhodobacter sphaeroides (*22*) and X-ray crystallographic analysis of *Paracoccus denitrificans* (*23*) and bovine heart oxidase (*24*) have provided data for the existence in subunit I of an input pathway (channel D) for the pumped protons (see also ref *25*) and a distinct input pathway for the vectorial protons consumed in the reduction of O_2 to H_2O (channel K). More recent mutational analysis of *R. sphaeroides* cytochrome *c* oxidase indicates, however, that channel K mediates only the translocation of the first two vectorial protons consumed in the reduction of the binuclear center to the peroxy intermediate, while channel D in addition to the four pumped protons would also translocate the two vectorial protons consumed in the conversion of the peroxy compound to the ferryl and this to the oxidized form of the binuclear center (*26*, *27*).

In the present work, eight protolytic residues in subunit I of the of aa_3-600 quinol oxidase were mutagenized to nonpolar residues. Only two of the mutations introduced, Y284F and K304L, resulted in definite effects on the activity of the enzyme. Both mutants, grown to the exponential phase in a rich medium, expressed an higher amount of heme *a* in the membrane as compared to the wild-type strain; however, their energy-conserving function was impaired. In the Y284F mutant the electron-transfer activity of the aa_3-600 quinol oxidase was completely abolished. In the K304L mutant the aa_3-600 quinol oxidase retained substantial electron-transfer activity, but proton pumping activity was almost completely suppressed. These results are discussed in terms of the role that the two mutated residues can have in the protonmotive activity of the oxidase.

MATERIALS AND METHODS

Bacterial strains and growth conditions, DNA methods, and genetic techniques used for the general strategy of mutagenesis have already been described (*15*).

The site-directed mutagenesis on the *qoxB* gene was performed on the *Kpn*I−*Sph*I fragment of 835 bp subcloned in pTZ18 (Pharmacia). The *ung*, *dut E. coli* strain RZ1039 was used to produce uracil containing single-stranded DNA of this recombinant plasmid, and the site-directed mutations were obtained by using the appropriate oligonucleotides, as described by Kunkel et al. *(28)*. The mutagenized *Kpn*I−*Dra*III fragment (for a detailed restriction map of the constructed plasmids see ref *15*) was sequenced to verify the absence of any other mutation. The *Kpn*I−*Dra*III fragment of plasmid pDIA5343 (*15*) was finally replaced by the mutant copies from the constructs in pTZ18 (Pharmacia). The mutant strains of *B. subtilis* carrying the described mutations were constructed by using the replacement step of the strategy of mutagenesis previously described (*15*).

For preparation of solubilized membranes, 0.5 L cultures of *B. subtilis* wild-type and mutant strains were grown in 2 L flasks at 37 °C, and for the mutant strains overnight precultures were made in the presence of the required antibiotics. The bacterial cells were harvested during the exponential phase (OD_{600} = 0.7−0.9), and detergent-solubilized membranes were prepared as in Villani et al. (*15*). Optical spectroscopy and estimation of heme contents were performed as already described (*15*). For CO-reduced minus reduced difference spectra the reduced form of the membranous cytochromes was obtained by addition of a few grains of dithionite, and the room temperature spectra were stored in the memory of a diode array spectrophotometer. CO was then bubbled through the suspension (supplemented with a small amount of antifoam) for 2 min in the dark, the CO-reduced spectra were taken, and the stored reduced spectra were subtracted from it. The CO-reduced species were spectrally stable for at least 1 h.

For oxygen consumption measurements, the harvested bacteria were resuspended to an OD_{600} of 10 in LB (Luria−Bertani) medium, and 50 μL of this cell suspension was added to 1.6 mL of the same medium previously equilibrated at 37 °C for the polarographic measurement of the respiratory activity.

Proton translocation was measured electrometrically by the oxygen pulse method. Fifty milliliters of cells at the log growth phase was centrifuged and the pellet resuspended in 0.2 mL of the assay medium. Then 0.1 mL of this cell suspension was added to 3.1 mL of 50 mM KCl, 100 mM KSCN, and 0.5 mM Hepes (pH 7.4), in a stoppered glass vessel equipped with a Clark-type oxygen electrode and a fast responding pH electrode. The suspension was thermostated at 25 °C and vigorously stirred. The oxygen uptake by endogenous respiration was monitored until full anaerobiosis was achieved; after 5 min equilibration the pH of the suspension was 6.5−6.7, and proton release was elicited by addition of 2.5 μM O_2 as air-equilibrated bidistilled water at 25 °C; pH changes were quantitated by titrated 10 mM HCl additions.

For KCN titration of endogenous respiration, bacteria were harvested during the log growth phase, and the pellet was resuspended in a small volume of 50 mM Tris-HCl, pH 7.4, containing 50 mM NaCl. The cell suspension was then equally split into two 1.5 mL stoppered glass vessels equipped with Clark-type oxygen electrodes containing the same buffer equilibrated at 37 °C, and KCN titration was done essentially as described (*29*).

To obtain the aa_3-600 enriched fractions, solubilized membranes were prepared as previously described (*15*) except that Nonidet P40 (LKB) was used as a solubilizing detergent at a concentration of 3 mg/mg of protein. The solubilized membranes were then applied to a DEAE-Sephacel (Pharmacia) previously equilibrated with 20 mM Tris-HCl, 0.2 mM EDTA, and 0.1% *n*-dodecyl β-maltoside (Calbiochem). The elution was done by applying a 0−0.5 M NaCl gradient with the same buffer, the aa_3-600 being eluted around 0.4 M NaCl. The aa_3-600 fractions were finally concentrated in Centrispeed C30KD (MST).

The catalytic activities of the wild-type and the Y284F and K304L aa_3-600 mutagenized enzymes were measured at 25 °C in a 280 μL stoppered plexiglass vessel equipped with a Clark-type oxygen electrode, in a 50 mM phosphate buffer, pH 7.4, containing 1% *n*-dodecyl β-maltoside. Tetrachlorohydroquinone ($TCQH_2$) (from Sigma) was used as an electron donor, and enzymatic oxygen consumption was determined by subtracting HOQNO- (2-heptyl-4-hydroxyquinoline) and/or KCN-insensitive activity. For the KCN titration, equal amounts of the enzymes were incubated in the vessel in the above medium alone or supplemented with different concentrations of KCN. Then 0.5 mM $TCQH_2$ was added to the reaction mixture, and the initial rate of oxygen

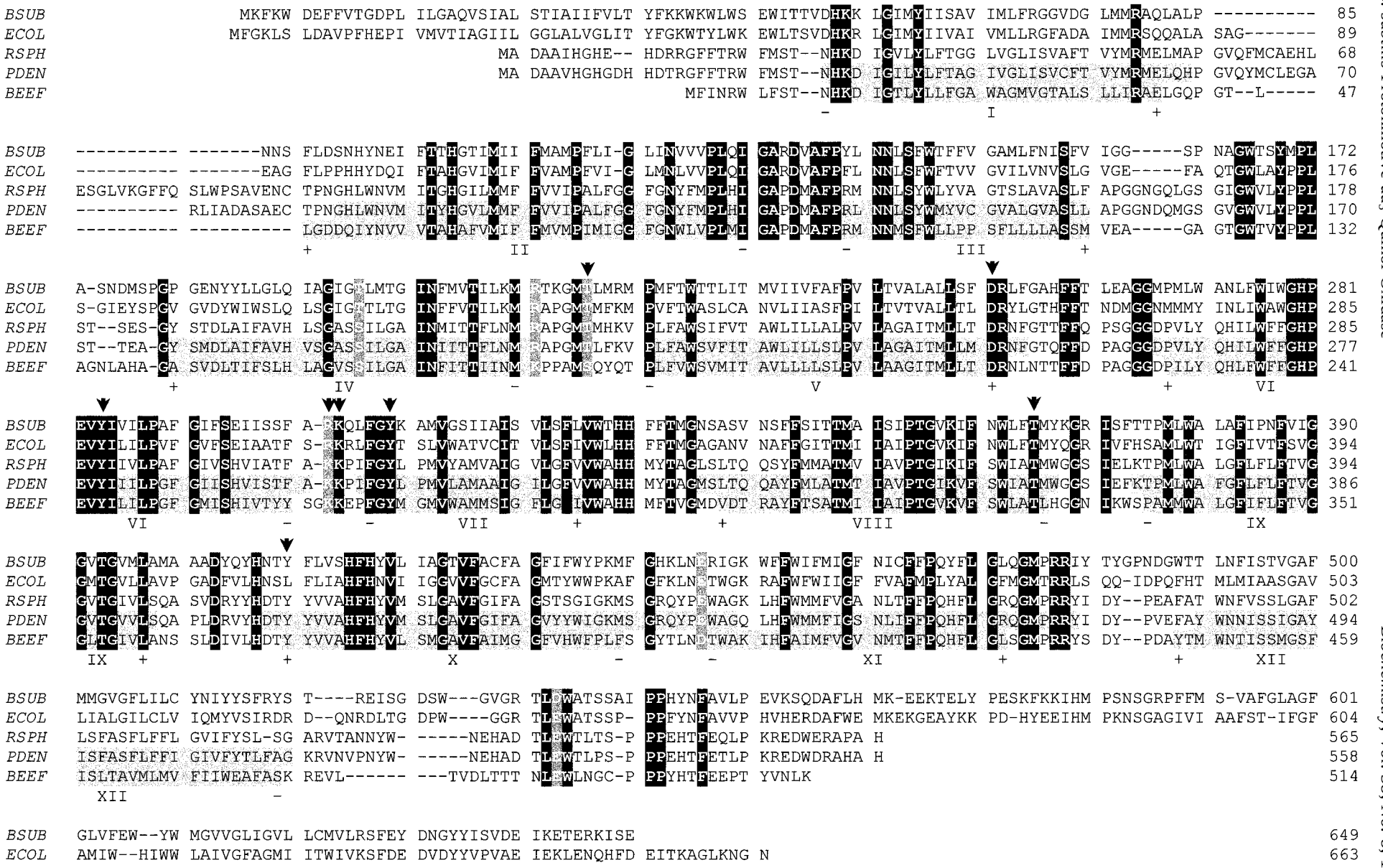

FIGURE 1: Sequence alignment of heme−copper oxidase subunit I: ECOL, *E. coli* bo_3 quinol oxidase; BSUB, *B. subtilis* aa_3-600 quinol oxidase; RSPH, *R. sphaeroides* cytochrome *c* oxidase; PDEN, *P. denitrificans* cytochrome *c* oxidase chain I β; BEEF, beef heart cytochrome *c* oxidase. The residues of *B. subtilis* aa_3-600 quinol oxidase mutagenized in the present work are indicated by arrows. Invariant or functionally conserved residues are shown in white on black and dark gray boxes, respectively. Transmembrane α-helices are boxed in gray with the (−) and (+) sign for the N and P side, respectively.

Table 1: Phenotypical Characterization of Wild-Type and Mutant Strains of *B. subtilis*[a]

	part A						part B			
	B.s. 168::spec^R	K304L	R303L	D252N	T217A	T365A	wild type	Y284F	Y309F	Y410F
heme *a*[b]	0.23	0.41	0.23	0.22	0.25	0.22	0.35	0.44	0.30	0.19
heme *b*[b]	0.28	0.33	0.32	0.24	0.31	0.34	0.71	0.36	0.70	0.75
heme *c*[b]	0.06	0.07	0.03	0.07	0.06	0.04	nd	0.20	nd	nd
O_2 consum[c]	179 ± 9	158 ± 10	165 ± 15	161 ± 10	177 ± 5	169 ± 11	182 ± 6	82 ± 3*	182 ± 17	154 ± 11
H^+/e^-	2.0 ± 0.1	1.3 ± 0.1*[f]	2.0 ± 0.1	1.8 ± 0.2	1.9 ± 0.1	1.8 ± 0.1	2.0 ± 0.05	1.2 ± 0.1*	2.0 ± 0.05	2.0 ± 0.05
$t_{1/2}$ (s^{-1})	9	9	12	8	9	9	15	15	18	18
power output[d]	360	212	323	286	337	300	365	115	364	308
strept res[e]	−	++	−	−	−	−	−	+++	−	−

[a] Heme content in detergent-solubilized membranes, respiratory rates, and redox-linked proton translocations in cell suspensions were measured as described in Materials and Methods. Parts A and B refer to the two experiment sets shown in Figures 2 and 3. [b] nmol of heme/mg of membrane proteins. [c] μM e^- min^{-1} $OD_{600}{}^{-1}$. [d] μM H^+ min^{-1} $OD_{600}{}^{-1}$. [e] Streptomycin resistance tested in a range of 10−100 mg/L. [f],*Statistically significant, $P < 0.01$ as compared to the control; number of experiments, 4−8.

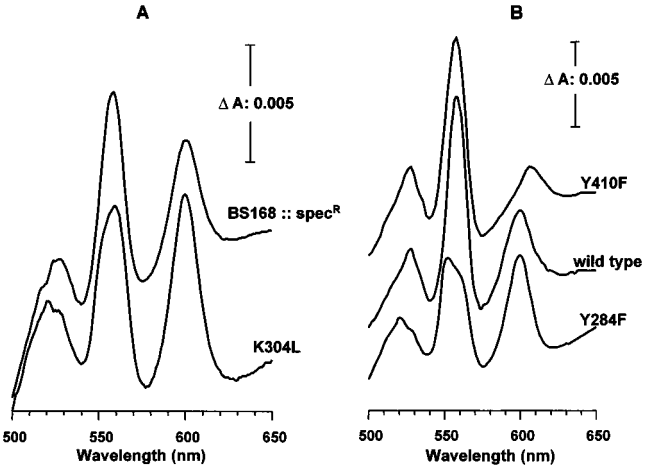

FIGURE 2: Difference optical spectra (dithionite reduced minus ferricyanide oxidized) of detergent-solubilized membranes of wild type and the mutant strains of *B. subtilis*. For experimental details see ref *15*. Spectra were scanned at a protein concentration of 1 mg/mL. (A) *B. subtilis* 168 was used as the wild-type strain and Triton X-100 was used as the solubilizing detergent. (B) *B. subtilis* 168::Spec^R (*15*) was used as the control strain and *n*-dodecyl β-maltoside was used as the solubilizing detergent. For other details see Materials and Methods.

consumption was measured and expressed as a percentage of the uninhibited activity.

RESULTS

By means of the mutagenesis strategy previously described, based on a two-step gene replacement method, site-directed mutations of the *qoxB* gene (encoding for subunit I of the aa_3-600 quinol oxidase) of *B. subtilis* were directly introduced in the bacterial chromosome. Figure 1 shows an alignment of the primary sequences of subunits I of *B. subtilis* aa_3-600 quinol oxidase, *E. coli* bo_3 quinol oxidase, and beef heart, *P. denitrificans*, and *R. sphaeroides* cytochrome *c* oxidases with the position of the conserved amino acid residues of the aa_3-600 quinol oxidase that were mutagenized indicated by arrows. The following mutants were constructed (see Table 1): T217A, D252N, Y284F, R303L, K304L, Y309F, T365A, and Y410F.

In Figure 2 the difference spectra of solubilized membranes of the wild type and some of the mutant strains of *B. subtilis* are shown. The peak at 600 nm is indicative of the aa_3-type quinol oxidase of the wild-type strain of this bacterium (*30, 31*). This peak, which disappears in the Δqox strain (*15*), is then restored at the same position in all the mutant strains, with the exception of the Y410F mutant. In this strain the peak shows a blue shift of 5 nm, thus confirming what was previously found in the cytochrome *c* oxidase of *R. sphaeroides* (*32*).

Table 2: Kinetic Characterization of aa_3-600 Enriched Fractions and KCN Inhibition Properties of Wild-Type and K304L *B. subtilis* aa_3-600 Quinol Oxidases[a]

	B.s. 168::spec^R	K304L
V_{max} ($TN \cdot s^{-1}$)[b]	15.1	9.6
K_m (mM)[b]	1.2	1.6
in vitro KCN I_{50} (μM)[b]	13	34
in vivo KCN I_{50} (μM)[c]	33	66

[a] For experimental details see Materials and Methods. [b] Measured on aa_3-600 enriched fractions. [c] Measured on endogenous respiration of intact cells. I_{50} was obtained from the data reported in Figure 5.

Table 1 summarizes the results of the phenotypic characterization of the wild-type and mutant strains of *B. subtilis* produced in two separate sets of experiments (parts A and B). For a first rapid screening, the strains were grown in the presence of different concentrations of streptomycin. This antibiotic has been extensively used for the isolation of mutants which are defective in aa_3-type oxidase activity (*33*). The sensitivity to this antibiotic that was lost, as expected, in the Δqox strain (*15*) was fully restored in all the mutant strains with the exception of the K304L and Y284F mutants. Determination of the content of heme *a* in the membranes shows that the mutants Y284F and K304L overexpressed heme *a*; a depression was, on the other hand, found in the mutant Y410F. It has to be noted that, for the mutant Y410F, the same ϵ for the calculation of heme *a* concentration, even if the peak resulted blue-shifted by 5 nm, was used. The respiratory activities of the mutant strains were comparable to the wild-type strain except in the case of the mutant Y284F which showed a marked depression in the rate of O_2 consumption. The respiratory activity of the K304L mutant strain, when referred to the heme *a* content, resulted, however, in being depressed by 50% (compare with the results presented in Table 2). The redox-linked proton pumping activity, which was lost in the strain Δqox (*15*), was restored with stoichiometries close to that of the wild type in the mutants T217A, D252N, R303L, Y309F, T365A, and Y410F but was markedly depressed in the mutants Y284F and K304L (Table 1; see also Figure 3). The lower stoichiometry in the proton pumping activity of these two strains was not associated with an increase of the $t_{1/2}$ of the

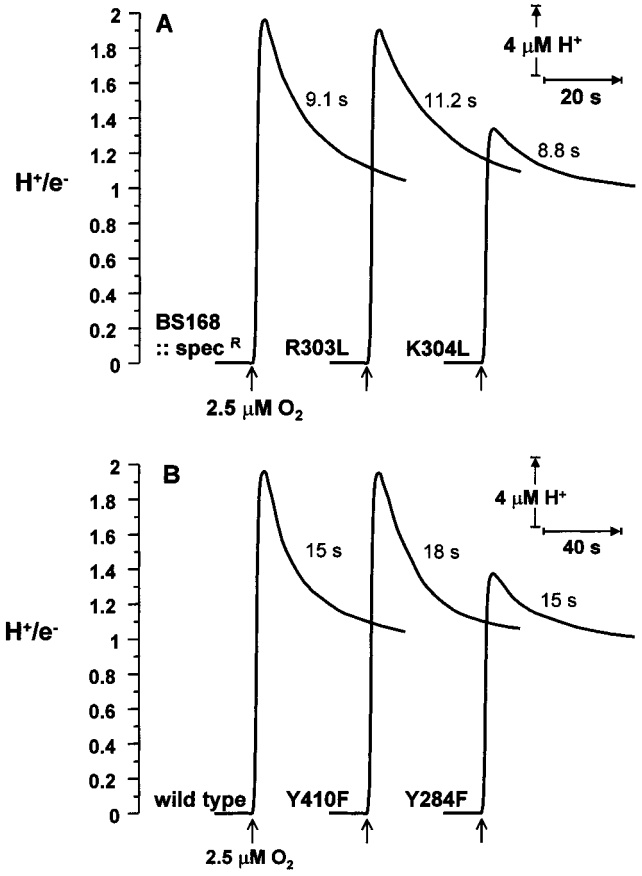

FIGURE 3: Redox-linked proton translocation measured in intact cells of wild type and the mutant strains of *B. subtilis*. For experimental conditions see ref *15*. Panels A and B refer to the two experiment sets shown in Figure 2. The numbers on the curves refer to the $t_{1/2}$ of the proton back-flow following the initial proton release. For experimental details see Materials and Methods.

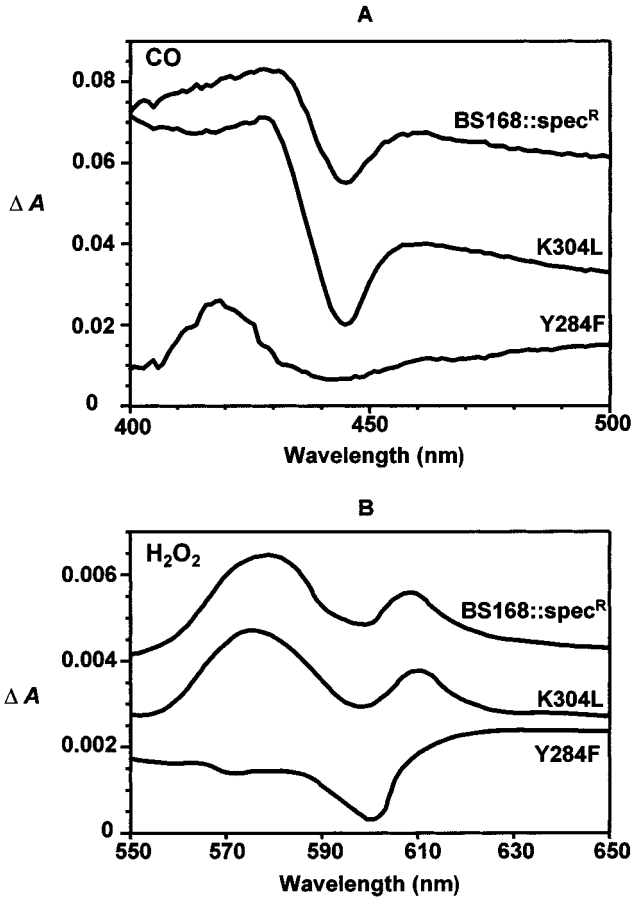

FIGURE 4: Difference spectra of (A) CO-reduced minus reduced and (B) H_2O_2-supplemented minus oxidized solubilized membranes from wild type and mutant strains of *B. subtilis*. Detergent-solubilized membranes were suspended at a final concentration of 2 mg of protein/mL and spectra recorded as in ref *15*. (A) See Materials and Methods. (B) Oxidized membranous aa_3-600 quinol oxidases were incubated with 0.5 mM H_2O_2 at pH 8.0 for 30 s (*32*) after which the difference spectra were recorded.

proton back-flow after the external acidification elicited by the oxygen pulse of the anaerobic bacterial suspension (Figure 3). To exclude the possible occurrence of secondary mutations, two independently isolated clones, Y284F*bis* and K304L*bis*, were analyzed. These clones showed the same phenotypic pattern of their counterparts as far as streptomycin resistance, spectra on solubilized membranes, and proton translocation stoichiometries were concerned (data not shown).

Figure 4 shows the analysis in the wild-type and the Y284F and K304L mutant strains of the CO-reduced minus reduced and the H_2O_2 minus fully oxidized difference spectra performed on detergent-solubilized membranes. In the CO difference spectra (Figure 4A), the positive contribution of heme a_3 at 430 nm and the negative contribution at 444 nm [completely absent in the Δqox strain (*15*)] are present in the wild-type and in the K304L membranes, whereas they are clearly perturbed in the strain Y284F. Treatment of the solubilized membranes of the wild-type and the K304L strains with a limited amount of H_2O_2 (Figure 4B) resulted in steady-state formation of the peroxy and ferryl intermediates with absorbance maxima at 580 and 607 nm, respectively (*34*). This typical spectral pattern, occurring as a consequence of the peroxidase activity at the heme a_3-Cu_B binuclear center, was strongly altered in the Y284F strain.

Aerobic growth of *B. subtilis* 168 to the exponential phase in rich media results in constitutive expression of aa_3-600 quinol oxidase (*15*). Lack of significant expression of *d*-type oxidase, which has an absorption peak at 630 nm, is confirmed by the difference spectra presented in Figure 2. Absence of significant oxidase activity with ascorbate plus TMPD excluded the presence of the caa_3-605 cytochrome *c* oxidase. To exclude interference from nonpumping, *b*- (or *o*-) type quinol oxidase, which appears, however, to be expressed when the *qox* operon is deleted [see strain Δqox (*15*)], the respiratory activities of the wild-type strain and of the K304L mutant strain, were titrated with KCN. It should be pointed out at this point that the wild-type strain does not display a functional alternative oxidase (*15*). The results of this titration presented in Figure 5 show a somewhat lower sensitivity to KCN of the respiratory activity of the K304L strain as compared to the wild-type strain. It is worth noting that the logarithmic curves best-fitting the points of the in vivo KCN titration do not extrapolate to the value of 100% of respiratory activity in the absence of KCN. This is due to the sigmoidal shape of inhibitor titration curves of respiratory fluxes when the titrated enzyme is not rate limiting (*29, 35*). The slight difference in sensitivity of respiratory activities to inhibition by KCN between wild-type and K304L strains could be caused by several factors such as (i) possible contribution of the alternative oxidase (in this case, however, a double hyperbolic phase would have been expected in the

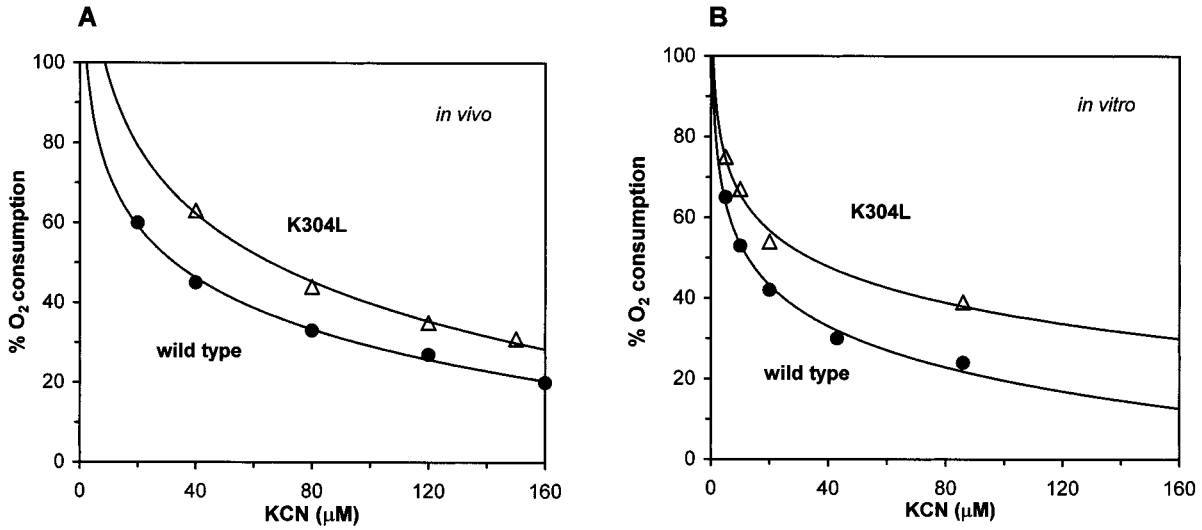

FIGURE 5: KCN titration of oxygen consumption in intact cells and aa_3-600 enriched fractions of *B. subtilis* 168::Spec^R and K304L strains. (A) KCN titration of endogenous respiration of *B. subtilis* 168::Spec^R (●) and K304L (△) strains. (B) KCN titration of $TCQH_2$ (tetrachlorohydroquinone) oxidation activity of aa_3-600 enriched fractions from *B. subtilis* 168::Spec^R (●) and K304L (△) strains. For experimental details see Materials and Methods.

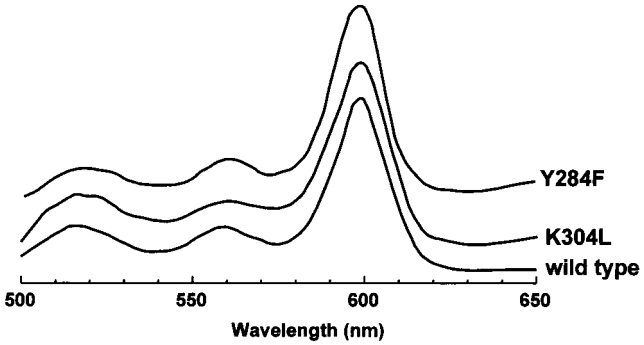

FIGURE 6: Difference optical spectra of aa_3-600 enriched fractions from *B. subtilis* 168::Spec^R, Y284F, and K304L strains. For details see Materials and Methods.

KCN titration curve; cf. Figure 5A and see ref *36*), (ii) different sensitivity to KCN of the two aa_3-600 oxidases, and (iii) higher relative maximum capacity of the aa_3-600 in the strain K304L (as compared to the wild-type strain), which would result in a shift of the inhibition threshold (*29*). To discriminate among these possibilities, we prepared aa_3-600 enriched fractions from the wild-type and the K304L strains. Figure 6 shows the difference spectra of these two preparations, indicating that there was in both preparations only a small and equivalent contribution of the *b*-type cytochromes.

In Table 2 the results of the analysis of the catalytic properties of the wild-type and the K304L aa_3-600 oxidases are reported. The aa_3-600 quinol oxidase of *B. subtilis* uses as endogenous substrate menaquinol-7, and the highest turnover numbers for this enzyme are obtained with the artificial substrate tetrachlorobenzoquinol ($TCQH_2$) (*30*). The mutant enzyme had a slightly lower affinity for the artificial substrate $TCQH_2$ and a reduced V_{max} as compared to the wild-type enzyme. The decrease in the specific respiratory activity relative to the heme *a* content of the mutant preparation as compared to the wild-type preparation was, on a percentage basis, practically the same as that observed for the mutant vs wild-type intact cells (Table 1). This excludes any difference in the relative maximum capacity of the aa_3-600 enzyme in the two strains. An aa_3-600 enriched fraction was also prepared from the Y284F mutant (see Figure 6). This fraction did not exhibit any quinol oxidase activity. Thus the residual respiratory activity exhibited by the intact Y284F mutant cells has to be ascribed, in this case, to alternative nonpumping quinol oxidases and/or to a small contribution of the cytochrome *c* respiratory branch. This (these) could come into action when, due to the suppression of the aa_3-600 quinol oxidase, the steady-state level of endogenous quinol increases. Figure 5B shows the KCN titration curves of the wild-type and K304L aa_3-600 quinol oxidases. In this case, the logarithmic best-fitting equations do extrapolate to 100% activity in the absence of KCN. In the conditions used for the determination of the respiratory activity in the enriched oxidase fractions, the enzyme is titrated as the isolated rate-limiting step. The K304L enzyme preparation shows a small decrease in the sensitivity to cyanide as compared to the wild-type enzyme, practically to the same extent as that observed in the intact cells. These results indicate that in the K304L mutant strain the respiratory activity of the cells is completely supported by the mutant K304L aa_3-600 quinol oxidase.

DISCUSSION

Of the eight mutations of protolytic to nonpolar residues we have introduced in subunit I of aa_3-600 quinol oxidase of *B. subtilis*, only two, namely Y284F and K304L, impaired the bioenergetic function of the microorganism as revealed by the appearance of the streptomycin resistance which appears to be directly correlated with the extent of power output (see Table 1). The Y284F mutation suppressed the electron-transfer activity of the aa_3-600 quinol oxidase of *B. subtilis*, as already observed for this mutation in the *bo* quinol oxidase of *E. coli* (*37*−*39*). The Y284F mutation did not alter the reduced (dithionite) minus oxidized (ferricyanide) difference spectrum of aa_3 (Figures 2 and 6) but perturbed the interaction of a_3 with CO and suppressed the production of the peroxy and ferryl compounds by added H_2O_2 (Figure 4). X-ray crystallographic analyses of aa_3 cytochrome *c* oxidase of *P. denitrificans* (*40*) and of bovine

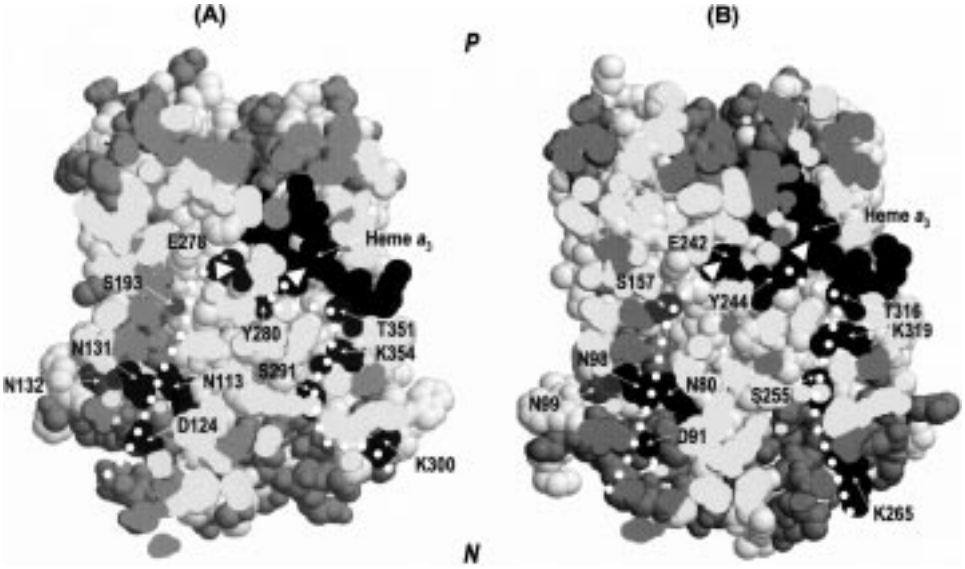

FIGURE 7: Space-filling view of a cross section parallel to the membrane of subunit I of *P. denitrificans* (A) and bovine heart (B) cytochrome *c* oxidase. Data are from the PDB coordinates of the crystal structures of the *P. denitrificans* (*23*) and bovine heart oxidase (*24*), drawn using the RasMol 2.6 program. Heme a_3 and conserved protolytic residues involved in the proton conduction pathways (channels D and K, indicated by white dotted arrows) are shown in black. The polar residues (in gray) and cavities connecting the protolytic residues are also made visible. P and N indicate the outer and inner aqueous phases, respectively. For other details see the text.

heart mitochondria (*41*) show that the conserved tyrosine in the position corresponding to Y284 of the *B. subtilis* quinol oxidase (Y280 in the *P. denitrificans* and Y244 in bovine heart) is covalently bound to one (H276 in *P. denitrificans*, H240 in bovine heart, H280 in *B. subtilis*) of the three conserved histidines which serve as ligands to Cu_B. On the basis of crystallographic analyses, it has also been proposed that Y280 of the *P. denitrificans* oxidase (*23*) and the corresponding Y244 in the bovine heart oxidase (*24*) are located at the inner end of the putative channel in subunit I, which would transfer the scalar protons consumed in the reduction of O_2 to $2H_2O$ from the inner aqueous phase to the binuclear center. This proton-transfer pathway (channel K) involves a conserved lysine (K354 in *P. denitrificans*, K319 in bovine heart) of subunit I (*23, 24*) (Figure 7). Mutation of this lysine to methionine in prokaryotic cytochrome *c* oxidases indicates, however, that this residue is involved in the initial reduction of the binuclear center to the peroxy compound(s), and the associated proton uptake, but not in the uptake of vectorial and pumped protons associated to the reactions leading from the peroxy compounds onward (*26, 27*).

The K304L mutation, which we have introduced in the aa_3-600 quinol oxidase of *B. subtilis*, causes partial inhibition of the electron-transfer activity of the enzyme, does not alter the reduced minus oxidized difference spectrum of aa_3, and does not affect the reaction of the binuclear center with CO and H_2O_2. It causes, on the other hand, substantial suppression of the pumping activity of the quinol oxidase and induces streptomycin resistance. This lysine residue is located in the loop connecting helices VI and VII at the inner (N) surface of the enzyme (Figure 7), in a position which is conserved (as K or R) practically in all the heme−copper oxidases so far sequenced (see Figure 1). It may be significant that the mutation R303L does not have any effect on the aa_3-600 quinol oxidase. It seems possible to conclude that the conserved K304 is essential for the proton pumping activity of the oxidase. The crystal structures of the *P. denitrificans* (*23*) and bovine heart oxidases (*24*) show that this lysine (K300 in the *P. denitrificans*, K265 in bovine cytochrome *c* oxidase) is exposed to the inner aqueous space (N side). In the bovine as well as in the *P. denitrificans* oxidase the conserved lysine is apparently connected to the conserved S255 (bovine; S291 in *P. denitrificans*) of the K channel but is far away from the conserved D91 and N98 (bovine; D124 and N131 in *P. denitrificans*) which are considered to be essential components of the entry mouth of channel D of pumped protons (*20*−*24*). It is interesting to note that in the bovine oxidase crystal the peripheral extensions of the supernumerary subunits cover all the conserved protolytic residues at the N surface of subunit I, except D91 and K265 which remain exposed to the bulk water (see refs *24* and *42*).

It has been proposed that in the bovine oxidase K265 is located at the entrance of the K channel, being connected to the conserved S255 and K319 (bovine; S291 and K354 in *P. denitrificans*) by protolytic residues (T489, T490, N491, H256) with intercalated hydrogen-bonded water molecules (Figure 10C in ref *24*) (Figure 7). The above protolytic residues are not all conserved in the *P. denitrificans* cytochrome *c* oxidase and *B. subtilis* aa_3 quinol oxidase. Inspection of the crystal structure shows, however, that there are also in *P. denitrificans* oxidase additional protolytic residues which, possibly with intercalated H_2O molecules (cf. ref *43*), can provide protonic connectiveness of K300 with S291, K354, T351, and Y280, conserved residues of the K channel (Figure 7). Furthermore, it is apparent from the space-filling view of cross sections of the two crystal structures (Figure 7) that there are cavities which could be filled by water molecules establishing secondary protonic connectiveness of K265 (bovine; K300 in *P. denitrificans*) and S255 (bovine; S291 in *P. denitrificans*) with conserved protolytic residues in the D channel (Figure 7).

It seems possible to conclude that the conserved K304 we have mutated to L in the *B. subtilis* quinol oxidase is a component of the entry mouth of the K channel. The presence

of additional protolytic residues around this conserved lysine, as well as its possible protonic connectiveness with protolytic residues of the D channel, seems to explain why the mutation K304L causes only partial inhibition of the steady-state activity of the oxidase but marked depression of the proton pumping, at difference of the replacement of the conserved lysine corresponding to K319 in the bovine and K354 in the *P. denitrificans* oxidase (*26*, *44*, *45*) which results in complete suppression of the steady-state oxidase activity. Impairment of the translocation of the vectorial protons, apparently only the first two consumed in the formation of the peroxy compound (*26*, *27*), can result in short circuit of the protons moving in the D channel to the binuclear center where they will be consumed in the chemistry of reduction of O_2 to H_2O with impairment of proton pumping. The present observations would suggest that the utilization of the D and K channel for the translocation of pumped protons and those used in the various steps of the reduction of O_2 to H_2O is not strictly specific. In particular, the D channel, which appears to be used for pumped protons, could also serve for translocation of vectorial protons in the P → F and F → O steps of the chemistry of oxygen reduction (*26*, *27*) as well as in the O → P step, at least in the particular conditions as those introduced by the mutation K304L we have described here.

ACKNOWLEDGMENT

We thank Michele Minuto for the construction of the plexiglass microvessel used in the oxygen consumption measurements.

REFERENCES

1. Saraste, M. (1990) *Q. Rev. Biophys. 23*, 331−336.
2. Garcia-Horsman, J. A., Barquera, B., Rumbley, J., Ma, J., and Gennis, R. B. (1994) *J. Bacteriol. 176*, 5587−5600.
3. Mitchell, P. (1966) Glynn Research Ltd., Bodmin, U.K.
4. Papa, S. (1988) in *Oxidases and Related Redox Systems* (Mason, H. S., Ed.) pp 49−94, Elsevier, Amsterdam.
5. Babcock, G. T., and Wikström, M. (1992) *Nature 356*, 301−309.
6. Papa, S. (1976) *Biochim. Biophys. Acta 456*, 39−84.
7. Wikström, M. (1977) *Nature 266*, 271−273.
8. Wikström, M., Krab, K., and Saraste, M. (1981) *Annu. Rev. Biochem. 50*, 623−655.
9. Kadenbach, B., Jaraush, S., Hartmass, R., and Merle, P. (1983) *Anal. Biochem. 129*, 517−521.
10. Kunst, F., et al. (1997) *Nature 390*, 249−256.
11. von Wachenfeldt, C., and Hederstedt, L. (1992) *FEMS Microbiol. Lett. 100*, 91−100.
12. De Vrij, W., Van den Burg, B., and Konings, W. N. (1987) *Eur. J. Biochem. 166*, 589−595.
13. James, W. S., Gibson, F., Taroni, P., and Poole, R. K. (1989) *FEMS Microbiol. Lett. 58*, 277−282.
14. De Gier, J.-W. L., Lubben, M., Reijnders, W. N. M., Tipker, C. A., Slotboom, W. N. M., Van Spanning, R. J. M., Stouthamer, A. H., and Van der Oost, J. (1994) *Mol. Microbiol. 13*, 183−196.
15. Villani, G., Tattoli, M., Capitanio, N., Glaser, P., Papa, S., and Danchin, A. (1995) *Biochim. Biophys. Acta 1232*, 67−74.
16. Santana, M., Kunst, F., Hullo, M. F., Rapoport, G., Danchin, A., and Glaser, P. (1992) *J. Biol. Chem. 267*, 10225−10231.
17. Presecan, E., Moszer, I., Boursier, L., Cruz Ramos, H., de la Fuente, V., Hullo, M.-F., Lelong, C., Schleich, S., Sekowska, A., Song, B. H., Villani, G., Kunst, F., Danchin, A., and Glaser, P. (1997) *Microbiology 143*, 3313−3328.
18. Haltia, T., Saraste, M., and Wikström, M. (1991) *EMBO J. 10*, 2015−2021.
19. Saiki, K., Nakamura, H., Mogi, T., and Anraku, Y. (1996) *J. Biol. Chem. 271*, 15336−15340.
20. Thomas, J. W., Puustinen, A., Alben, J. O., Gennis, R. B., and Wikström, M. (1993) *Biochemistry 32*, 10923−10928.
21. Garcia-Horsman, J. A., Puustinen, A., Gennis, R. B., and Wikström, M. (1995) *Biochemistry 34*, 4428−4433.
22. Fetter, J. R., Qian, J., Shapleigh, J., Thomas, J. W., Garcia-Horsman, A., Schmidt, E., Hosler, J., Babcock, G. T., Gennis, R. B., and Ferguson-Miller, S. (1995) *Proc. Natl. Acad. Sci. U.S.A. 92*, 1604−1608.
23. Iwata, S., Ostermeier, C., Ludwig, B., and Michel, H. (1995) *Nature 376*, 660−669.
24. Tsukihara, T., Aoyama, H., Yamashila, E., Tomizaki, T., Yamagushi, H., Shinzawa-Itoh, K., Nakashima, R., Yaono, R., and Yoshikawa, S. (1996) *Science 272*, 1136−1144.
25. Verkhovskaya, M. L., Garcia-Horsman, A., Puustinen, A., Rigaud, J. L., Morgan, J. E., Verkhovsky, M. I., and Wikström, M. (1997) *Proc. Natl. Acad. Sci. U.S.A. 94*, 10128−10131.
26. Konstantinov, A. A., Siletsky, S., Mitchell, D., Kaulen, A., and Gennis, R. B. (1997) *Proc. Natl. Acad. Sci. U.S.A. 94*, 9085−9090.
27. Ädelroth, P., Gennis, R. B., and Brzezinski, P. (1998) *Biochemistry 37*, 2470−2476.
28. Kunkel, T. A., Roberts, J. D., and Zakour, R. A. (1987) *Methods Enzymol. 154*, 367−382.
29. Villani, G., and Attardi, G. (1997) *Proc. Natl. Acad. Sci. U.S.A. 94*, 1166−71.
30. Lauraeus, M., Haltia, T., Saraste, M., and Wikstrom, M. (1991) *Eur. J. Biochem. 197*, 699−705.
31. Lauraeus, M., Wikstrom, M., Varostis, C., Tecklenburg, M. M. J., and Babcock, G. T. (1992) *Biochemistry 31*, 10054−10060.
32. Hosler, J. P., Ferguson-Miller, S., Calhoun, M. W., Thomas, J. W., Hill, J., Lemieux, L. J., Ma, J., Georgiou, C., Fetter, J., Shapleigh, J., Tecklenburg, M. M. J., Babcock, G. T., anf Gennis, R. B. (1993) *J. Bioenerg. Biomembr. 25*, 121−136.
33. Taber, H. W., Mueller, J. P., Miller, P. F., and Arrow, A. S. (1987) *Microbiol. Rev. 51*, 439−457.
34. Vygodina, T. V., and Konstantinov, A. A. (1988) *Ann. N.Y. Acad. Sci. 550*, 124−138.
35. Letellier, T., Heinrich, R., Malgat, M., and Mazat, J.-P. (1994) *Biochem. J. 302*, 171−174.
36. Yaginuma, A., Tsukita, S., Sakamoto, J., and Sone, N. (1997) *J. Biochem. 122*, 969−976.
37. Thomas, J. W., Calhoun, M. W., Lemieux, L. J., Puustinen, A., Wikström, M., Alben, J. O., and Gennis, R. B. (1994) *Biochemistry 33*, 13013−13021.
38. Kawasaki, M., Mogi, T., and Anraku, Y. (1997) *J. Biochem. 122*, 422−429.
39. Mogi, T., Minagawa, J., Hirano, T., Sato-Watanabe, M., Tsubaki, M., Uno, T., Hori, H., Nakamura, H., Nishimura, Y., and Anraku, Y. (1998) *Biochemistry 37*, 1632−1639.
40. Ostermeier, C., Harrenga, A. Ermler, U., and Michel, H. (1997) *Proc. Natl. Acad. Sci. U.S.A. 94*, 10547−10553.
41. Yoshikawa, S., Shinzawa-Itoh, K., Nakashima, R., Yaono, R., Yamashita, E., Inoue, N., Yao, M., Fei, M. J., Libeu, C. P., Mizushima, T., Yamaguchi, H., Tomizaki, T., and Tsukihara, T. (1998) *Science 280*, 1723−1729.
42. Papa, S., Capitanio, N., and Villani, G. (1998) in *Frontiers of Cellular Bioenergetics: Molecular Biology, Biochemistry and Physiopathology* (Papa, S., Guerrieri, F., and Tager, J. M., Eds.) Plenum Press, London (in press).
43. Hofacker, I., and Schulten, K. (1998) *Proteins 30*, 100−107.
44. Vygodina, T. V., Pecoraro, C., Mitchell, D., Gennis, R., and Konstantinov, A. A. (1998) *Biochemistry 37*, 3053−3061.
45. Zaslavsky, D., and Gennis, R. B. (1998) *Biochemistry 37*, 3062−3067.

BI980774G